A Topological Analysis of the Space of Natural Images

Gunnar Carlsson
Tigran Ishkhanov*

Abstract

In this paper we study the Space of Natural Images locally. We apply the techniques of computational algebraic topology to the space of 3x3 and 5x5 high-contrast patches and show that in both cases the subspace of linear and quadratic gradient patches, which forms a dense subset inside the space of all high-contrast patches, possesses an interesting topological filtration and is itself topologically equivalent to the Klein bottle.

Keywords : topology; natural images; manifold; filtration; Klein bottle; persistent homology; high-contrast patches.

Introduction

Natural image statistics has attracted a lot of interest in the recent years. There have been a lot of successful attempts to approach this subject by researchers from areas as different as neuroscience and physiology on the one hand and computer vision on the other. In this paper we take up a "local" approach. That is, instead of looking at an image as a whole we analyze the structure of its high-contrast regions (pixel patches). While most of the work done in this direction concentrated on statistical properties of such "local" regions, we are interested in topology of this space or, more precisely, in topology of the space of n by n high-contrast pixel patches with sufficiently small n. The question about the existence of a manifold structure within a space of patches was raised in [10], where the authors study the global statistics of the space of 3 by 3 patches.

*e-mail addresses: gunnar@math.stanford.edu, tigran@math.stanford.edu

There are many advantages to analyzing a space of natural images locally. First, this greatly reduces the dimensionality of the problem. While the original image taken by the digital camera naturally lives in a very high-dimensional space (with the number of dimensions equals the number of pixels), a space of n by n patches can be viewed as a subspace of n^2-dimensional vector space. If n is small, and in our case $n = 3$ or 5, this is computationally tractable. Second, it has been observed by several authors ([5], [7]) that an understanding of the local statistics provides a lot of information about global statistical properties of the image; this is commonly referred to as scaling of the natural image statistics. And third, the results in [9] provide evidence that humans tend to focus more on the scale-invariant features of the image, while in [11] the authors report that humans look more in the regions with high spatial contrast when presented with a natural image scene.

The paper follows the topological line of research initiated in [2] and continued in [1]. We use sub and superlevel sets of a certain set of functions to cut out the subspace of linear and quadratic gradient patches that also constitute the densest subspace inside the 3 by 3 patch space. We also show that most of the results for 3 by 3 patches are valid in a 5 by 5 patch space as well.

0.1 Outline of the paper

The paper is organized as follows. In section 1 we give a brief theoretical and computatational account of algebraic topological methods that are used in this paper. Section 2 is dedicated to explanation of the details of the patch space construction. In the next section 3 we present the computational methods used in the paper. In section 4 we report our main results. Section 5 contains a summary and discussion of possible future directions of research. Most of the computational details are given in the Appendix.

1 Computational algebraic topology

1.1 Classical algebraic topology

Loosely speaking, topology aims at studying spaces in whole. Unlike geometry which concentrates on small neighborhoods of individual points to compute local invariants such as curvature, torsion etc. topology is concerned with more global information about the space. For example, one natural question to ask within a topological framework is whether

the space at hand is connected (any two points can be joined by a path within the space), yet another question might be whether any two paths between a fixed pair of points can be deformed into one another keeping the endpoints fixed. The "algebraic" in algebraic topology arises when we give our initial space some robust structure, e.g. the structure of a simplicial complex which we will discuss in more detail below or more generally the structure of a cell complex. For a friendly introduction to algebraic topology we refer reader to [6].

Classical algebraic topology deals with spaces consisting of an infinite set of points. Such a space can be defined by a set of equations or descriptively, e.g. the space of all unit vectors in $\mathbb{R}^3$. In our case we have spaces consisting of a finite collection of points so standard methods are not directly applicable. To deal with such situations computational algebraic topological methods were developed.

To enable algebraic methods we approximate our space of finitely many points by a combinatorial (rigid) structure known as simplicial complex. Our main computational invariant for a space is its homology groups, which have a particularly nice description within a simplicial framework. Intuitively, homology measures the number of "holes" of variuos dimensions a given space has. For example, one might say that a circle has exactly one one-dimensional hole, figure "8" has two and sphere has one two-dimensional hole. Indeed, this is exactly the information homology groups contain: one generator in first homology group of a circle, two in first homology group of figure "8" and one generator in the second homology group of a sphere. The number of generators of n-th homology group of a given space is called n-th Betti number of a space.

The combinatorial nature of simplicial complex allows one to compute its homology groups numerically once a particular simplicial approximation of the space is chosen. The question arises as to how to approximate a space of discrete points by a continuous object such as simplicial complex? In the next section we introduce a concept of persistent homology and explain how it helps to answer the above question.

1.2 Persistent homology

Before we introduce the notion of persistence we need to delve deeper into the subject of simplicial complexes.

Simplicial complexes are finite lists of simplices. Geometrically, a simplex can be described as follows. Given $n+1$ points in $\mathbb{R}^m$, the n-simplex is a convex body bounded by the union of $(n-1)$-linear sub-

spaces of $\mathbb{R}^m$ defined by all possible collections of n points (chosen out of $n+1$ points). For example, a 1-simplex is an interval, 2-simplex is a triangle, 3-simplex is a tetrahedron and so on. Simplices in simplicial complex overlap in a prescribed way, and the linear algebraic methods used to compute homology operate on vector spaces whose bases consist of collections of these simplices. The idea is to take a space $X \subseteq \mathbb{R}^n$, or rather a finite set of points $\mathbb{X}$ sampled from X, together with a parameter ϵ, and construct from it a simplicial complex, called the Vietoris-Rips complex, denoted $VR(\mathbb{X}, \epsilon)$. The complex will have $\mathbb{X}$ as its vertex set, and a collection $\{x_0, x_1, \ldots, x_k\}$ will span a k-simplex in $VR(\mathbb{X}, \epsilon)$ if and only if $d(x_i, x_j) \leq \epsilon$ for all $0 \leq i, j \leq k$, where d denotes the metric (distance), which is chosen depending on a problem at hand. When ϵ is very small, this still amounts to a discrete set of points, and when ϵ is large, it is a single simplex of dimension $\#(\mathbb{X}) - 1$ (provided $\mathbb{X}$ has more than one point). However, there is typically a middle range where $VR(\mathbb{X}, \epsilon)$ has homology isomorphic to that of X, and therefore has Betti numbers equal to those of X. When the space is a Riemannian manifold, for example, one can explicitly estimate a range of values of ϵ for which this is the case. However, in our case, when we only have the finite sample and no a priori information about the underlying space X, making such estimates is not possible. However, H. Edelsbrunner et al [4] have made the following observation. Given $\epsilon \leq \epsilon'$, there is a natural inclusion of simplicial complexes $VR(\mathbb{X}, \epsilon) \hookrightarrow VR(\mathbb{X}, \epsilon')$, and because of the functoriality property described above, one obtains a linear transformation $H_k(VR(\mathbb{X}, \epsilon)) \to H_k(VR(\mathbb{X}, \epsilon'))$ for any k. What Edelsbrunner et al observed was that in order to study the homology of a given space using a point cloud sampled from it, one should keep track of the entire system of vector spaces $H_k(VR(\mathbb{X}, \epsilon))$, together with all the linear transformations described above. Such a system will be called a *persistence vector space*, and it is shown in [14] that persistence vector spaces admit a classification analogous to the classification result for finite dimensional vector spaces, which asserts that two vector spaces of the same dimension are isomorphic. In the case of persistence vector spaces, it turns out that attached to each persistence vector space, there is an invariant called a *barcode* which is just a finite collection of intervals (perhaps infinite to the right), and that any two persistence vector spaces with the same barcodes are isomorphic. Figure 1 gives an example of a barcode for a figure "8". The interpretation of barcodes is that long intervals represent actual geometric structure of an underlying space from which the data is sampled, and shorter intervals are interpreted as noise. Of course, what

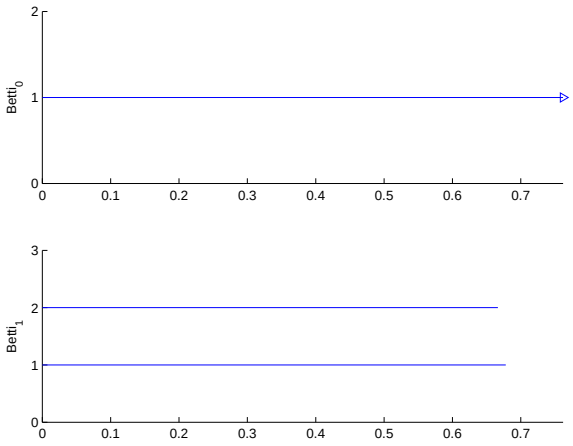

Figure 1: The barcode for the figure "8" space

is long and what is short depends on the nature of the problem, but the above statement is the guiding principle. Referring to figure 1 we see that there are two long lines in one-dimensional homology and one long line in 0-dimensional homology reflecting the fact that figure "8" has one connected component and two one-dimensional holes.

2 Space of patches

Our main space $\mathcal{M}$ is a collection of $4 \cdot 10^6$ '3 by 3' patches of high contrast obtained from the collection of still images gathered by H. van Hateren and A. van der Schaaf ([8]). $\mathcal{M}$ is a subset of a larger set $\tilde{\mathcal{M}}$, provided to us by K. Pedersen. The size of $\tilde{\mathcal{M}}$ is about $8 \cdot 10^6$. Below is a series of steps performed to obtain a set of high-contrast patches from a particular image. (See [10] for more details).

1. Select an image from the still image collection.
2. Extract at random 5000 3 by 3 patches from the image. Regard each patch as a vector in 9-dimensional space.
3. Next, for each patch do the following.
   (a) Compute the logarithm of intensity at each pixel.

(b) Subtract an average of all coordinates from each coordinate. This produces a new 9-vector.

(c) For this vector of logarithms compute the contrast or "D-norm" of the vector. The D-norm of a vector x is defined as $\sqrt{x^T D x}$, where D is a certain positive definite symmetric 9×9 matrix.

(d) Keep this patch if its D-norm is among the top 20 percent of all patches taken from the image.

4. Normalize each of the selected vectors by dividing by their respective D-norms. This places them on the surface of a 7-dimensional ellipsoid.

5. Perform a change of coordinates so that the resulting set lies on the actual 7-dimensional sphere in $\mathbb{R}^8$.

The space $\tilde{\mathcal{M}}$ was obtained by applying the above procedure to a subset of images from the still image collection.

3 Methods

In [1] it was shown that sublevel sets of density function defined on $\mathcal{M}$ have interesting and non-trivial topology for sufficiently high density thresholds. The density function used in that paper was F_k, whose value at a point p was defined as the inverse of a distance to the k-th nearest neighbor of p ([13]). A particular value of a parameter k does not matter as long as it is not too small to be affected by sampling noise.

To summarize the results of [1]: it was found that as density threshold f decreases the topology of the sublevel sets $F_k \geq f$ changes from a circle (linear intensity gradients) to a 3-circle space (linear gradients plus quadratic gradirents in vertical and horizontal directions) and finally becomes that of the Klein bottle (all linear and quadratic gradient patches) minus a certain measure 0 set D. We refer reader to [1] for in-depth explanation of why the sublevel sets have this particular topology. All patches in D are of the same nature, namely, they have diagonal pure quadratic gradients. Their relatively low density is partly due to the choice of patch shape as a square. This choice is influenced by technology - camera pixels form a grid with vertical and horizontal sides. And partly, is due to nature's preference for vertical and horizontal as opposed to intermediate directions.

We would like to obtain a similar topological filtration of $\mathcal{M}$ to the one in [1] but which wouldn't suffer from artifacts such as the camera's arrangement of pixels. We achieve such a filtration by using 3 naturally defined functions (which we call G, H and R) on $\mathcal{M}$. Let us also fix the notation g, h and r to denote the corresponding threshold values for each of these functions.

Each point of $\mathcal{M}$, i.e. each 3 by 3 patch can be thought of as lying in xy-plane with each of the nine pixels having coordinates $(x_0, y_0), x_0 \in \{-1, 0, 1\}, y_0 \in \{-1, 0, 1\}$. We denote the grid made by these nine points in a plane by Z. Let us also denote by I an intensity function on p. Note that given any function of two variables f (in particular, a polynomial), we can obtain a 3 by 3 patch by evaluating f on the 9 points of Z. The polynomial functions proved to be especially useful in explaining the topological results in [1] and we will turn to them later in this paper.

Let us now describe the construction of functions G, H and R. Most of the computational details of constructions presented in this section are given in the Appendix.

To define a function G on $\mathcal{M}$ we first compute the covariance matrix M of partial derivatives in x and y of intensity function I for a patch p

$$M = \begin{pmatrix} \int \frac{\partial I}{\partial x} \cdot \frac{\partial I}{\partial x} & \int \frac{\partial I}{\partial x} \cdot \frac{\partial I}{\partial y} \\ \int \frac{\partial I}{\partial x} \cdot \frac{\partial I}{\partial y} & \int \frac{\partial I}{\partial y} \cdot \frac{\partial I}{\partial y} \end{pmatrix}$$

Next, $G(p)$ is defined as an absolute value of the difference between eigenvalues of M, namely,

$$G(p) = |\lambda_{max} - \lambda_{min}|$$

The function G is designed to measure the directionality of a patch and thus we expect high-contrast linear gradient patches to have a high value of G.

The second function H is defined in two steps as well. First, we compute a hessian H_I of I at the central pixel of a patch, $H(p)$ is an absolute value of the largest eigenvalue of H_I, i.e.

$$H(p) = max(\gamma_1, \gamma_2)$$

The function H is designed to differentiate between quadratic and linear gradient patches. Patches whose gradient is close to being linear should have a very small value of H.

Let S be the following basis consisting of linear and quadratic functions.

$$S = \{1, x, y, xy, x^2 - y^2, x^2 + y^2\}$$

We orthonormalize S to obtain a new basis, still denoted by S. The definition of the function R uses a representation of a patch in S. More precisely, we compute coefficients of p in S using the standard scalar product and let $p_s = \sum_{f_i \in S} c_i \cdot f_i$, where c_i are the computed coefficients and $f_i \in S$. Then we define

$$R(p) = ||p - p_s||$$

The main point behind defining the function R in this way is that both linear and quadratic gradient patches should be approximated well using just the functions from S.

We select a subspace $\mathcal{K}_{g,h,r}$, which depends on the choice of the threshold values for g, h and r using the three defined functions and applying the following formula to $\mathcal{M}$

$$\mathcal{K}_{g,h,r} = \{p : R(p) \leq r \wedge (G(p) \geq g \vee H(p) \geq h)\};$$

Thus, we would like to cut out the set of patches which are well approximated by the set of functions in the basis B and either have strong directionality bias (linear gradient patches) or have a large eigenvalue of a Hessian at the central pixel (quadratic gradient patches). It is the spaces of the form $\mathcal{K}_{g,h,r}$ which we use in our subsequent topological analysis. In the next section we will see that in fact only a threshold for the function H needs to be changed to produce the family of topologies as in [1], the other two thresholds are kept constant throughout the procedure.

The spaces $\mathcal{K}_{g,h,r}$ are typically very large (recall that the size of the whole space $\mathcal{M}$ is $4 \cdot 10^6$). Therefore, we need a way of reducing their size without distorting their topology. To accomplish this task, we again turn to functions. Roughly speaking, the idea is to replace points of $\mathcal{K}_{g,h,r}$ by the clusters of preimages of intervals $[a, b]$ under suitably chosen functions on $\mathcal{K}_{g,h,r}$. As an illustrative example, consider a simple space such as circle S^1 defined in the xy-plane in the usual way by the equation $x^2 + y^2 = 1$ and let $f : \mathbb{R}^2 \to \mathbb{R}$ be defined as projection onto the x-axis, i.e. $f(x, y) = x$. We break the range of f into a finite set of intervals

$$R_f = \{[x_1, x_2], [x_2, x_3], \ldots, [x_{n-1}, x_n]\}$$

Next, we cluster each set $f^{-1}[x_i, x_j]$ and replace each of the clusters with its mean point. Thus, total number of points equals total number of clusters across all intervals $[x_i, x_j]$. If there is more than one function used (as in all of our cases) producing a map of the form $X \to \mathbb{R}^n$, we

break up the range into n-parallelepipeds and follow essentially the same procedure as in 1-dimensional case.

We apply this procedure to spaces $\mathcal{K}_{g,h,r}$ using a pair of functions. One is the function G defined earlier, the other is a function Θ also defined on all of $\mathcal{M}$. Recall that the symmetric matrix M defined above can always be brought to a diagonal form by an orthogonal basis transformation. Such a transformation in $\mathbb{R}^2$ is completely described by a rotation by a fixed angle, which we denote by θ. The function Θ is defined as a function of this angle, more precisely

$$\Theta(p) = \sin^2(2\theta)$$

Following our reduction method for $\mathcal{K}_{g,h,r}$ we cluster the preimages of rectangles in $\mathbb{R}^2$ under the pair of functions $(G(p), \Theta(p))$. Last step is to replace points of $\mathcal{K}_{g,h,r}$ with mean points of the corresponding clusters. Let us denote the reduced space by $\tilde{\mathcal{K}}_{g,h,r}$. The choices of functions and a particular decomposition of their ranges into intervals for the clustering algoritm were dictated by the results obtained in the controlled case (when the choices were applied to the ideal Klein bottle space as constructed in [1] using a polynomial model).

In the next section we describe the experimental results of feeding the family of spaces $\tilde{\mathcal{K}}_{g,h,r}$ into our topological software PLEX and computing their $\mathbb{Z}_2$ homology groups in dimensions 0, 1 and 2.

4 Experimental Results

We describe below the topology of $\tilde{\mathcal{K}}_{g,h,r}$ for various values of thresholding parameters g, h and r. Let us also fix the notation for a threshold triple as (g, h, r).

At the level $(g, h, r) = (1.5, \infty, 0.02)$ we recover the circle of linear gradients S_1 (see figure 3). The barcode shows one line in 0-dimensional homology and one in 1-dimensional homology. In terms of 2-variable polynomial functions the space S_1 can be given as a set of linear polynomiails of the form $\{ax + by\}$ with $(a, b) \in S^1$ since our patches are contrast-normalised.

Lowering the threshold h on H to $(g, h, r) = (1.5, 0.88, 0.02)$ we recover the 3-circle model S_3 (figure 4) described in [2] and in more detail in [1]. This space consists of a pair of secondary circles (vertical and horizontal quadratic gradients) each of which intersects the primary circle (linear gradients) in exactly two points. The secondary circles do

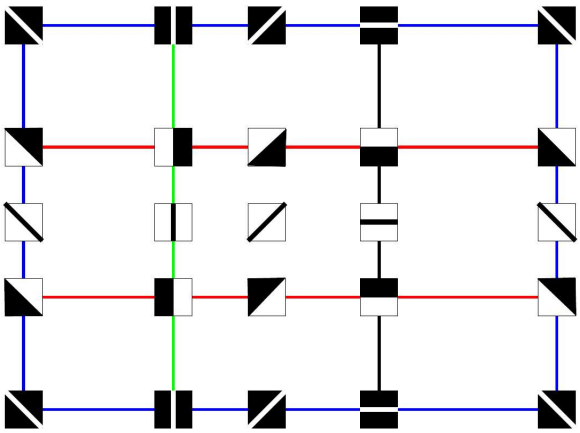

Figure 2: 3 by 3 patches parametrized by the Klein bottle

not intersect each other. The figure shows that the first Betti number is 5 in this case which is consistent with this model (as shown in [1]). The polynomial description for C_3 consists of the set of the form $c(ax + by)^2 + d(ax + by)$ with either $(c, d) = (0, 1)$, $(a, b) = (1, 0)$ or $(a, b) = (0, 1)$ giving the linear gradients circle, the vertical quadratic gradients circle and horizontal quadratic gradients circle respectively.

Finally, lowering h further to $(g, h, r) = (1.5, 0.8, 0.02)$ we obtain the Klein bottle's homology (figure 5). At this filtration level the space includes the 3-circle space and also quadratic gradients in all of the intermediate directions. The polynomial model for this space is given by all polynomials of the form $c(ax+by)^2+d(ax+by)$ with $(a, b) \in S^1$ and $(c, d) \in S^1$. It is proved in [2] that the space of polynomials of this form is indeed homeomorphic to the Klein bottle.

Figure 2 shows a space of patches parametrized by the Klein bottle. Here we use the standard representation of the Klein bottle with opposite horizonatal edges identified without orientation reversal and opposite vertical edges identified with orientation reversal. The circle of linear gradients is colored red (note that due to vertical edges identification it is in one connected component), and vertical and horizontal quadratic gradient patches are colored green and black respectively.

We repeated the same analysis using the same set of functions for the space of 5 by 5 patches. In this case it is possible to recover a 3-circle model and the Klein bottle but not the linear gradients circle. The results for the former two cases are presented on figure 6 and figure 7.

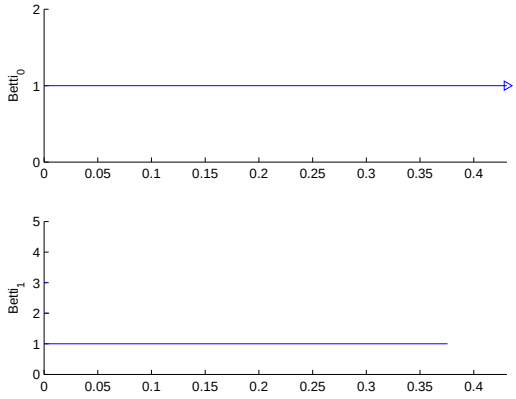

Figure 3: *PLEX* results for $\tilde{\mathcal{K}}_{1.5,\infty,0.02}$

At the level $(g, h, r) = (1.35, \infty, 0.15)$ we obtain a 3-circle model and at $(g, h, r) = (1.55, \infty, 0.15)$ - the Klein bottle.

5 Summary

We have shown that the space of high-contrast 3 by 3 patches with linear and quadratic gradients has a topological filtration whose second skeleton is topologically equivalent to a 2-manifold, the Klein bottle. We confirmed our findings by applying the same methods to the space of 5 by 5 patches. Together with the result in [1] that patches with linear and quadratic gradients have a high density in the space of all high-contrast patches, our results suggest that an efficient encoding of a large portion of a natural image is possible. Namely, instead of using an "ad hoc" dictionary for approximating high-conrast patches one can build such a dictionary in a systematic way by generating a uniform set samples from the ideal Klein bottle provided by the polynomial model.

Appendix

Here we give details of various computational procedures described in the main body of the paper.

To define a function $G(p)$ we need a discrete version of the gradient in x and y directions. To write down the formulas let us first fix some

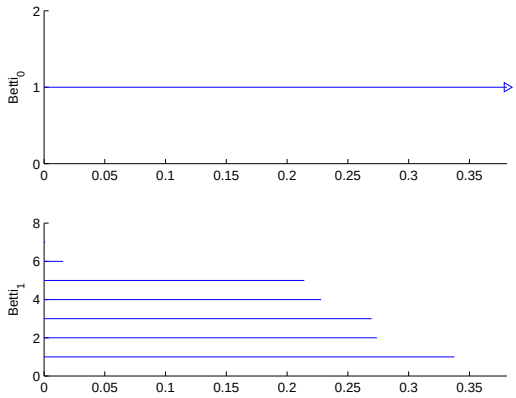

Figure 4: $PLEX$ results for $\tilde{\mathcal{K}}_{1.5,0.88,0.02}$

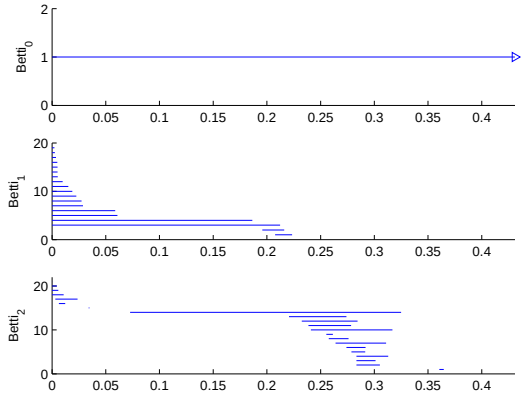

Figure 5: $PLEX$ results for $\tilde{\mathcal{K}}_{1.5,0.8,0.02}$

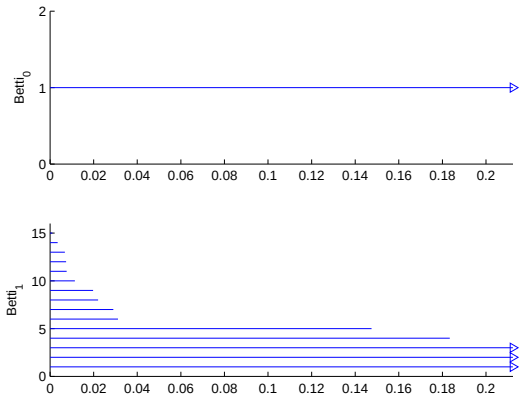

Figure 6: $PLEX$ results for $\tilde{\mathcal{K}}^{N=5}_{1.35,\infty,0.15}$

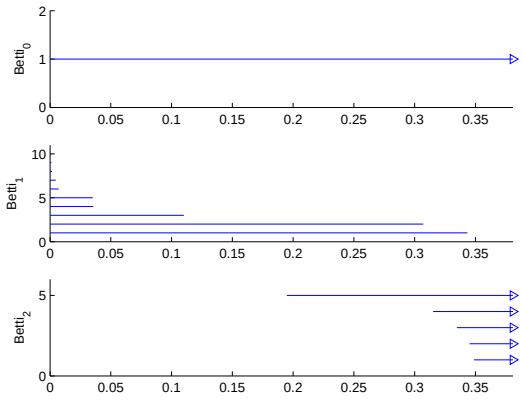

Figure 7: $PLEX$ results for $\tilde{\mathcal{K}}^{N=5}_{1.55,\infty,0.15}$

notation. For a patch p of size n by n we let $p(i,j)$ be the pixel whose x-coordinate is i and whose y-coordinate is j. We define a discrete version of partial derivative with respect to x (the formulas for partials with respect to y are similar) as

$$p_x(i,j) = p(i+1,j) - p(i,j), \quad if \quad i = -\lfloor n/2 \rfloor \tag{1}$$

$$p_x(i,j) = (p(i+1,j) - p(i-1,j))/2, \quad if \quad -\lfloor n/2 \rfloor < i < \lfloor n/2 \rfloor \tag{2}$$

$$p_x(i,j) = p(i,j) - p(i-1,j), \quad if \quad i = \lfloor n/2 \rfloor \tag{3}$$

Representing the matrix M (see section 3) in the form

$$\begin{pmatrix} A & B \\ B & C \end{pmatrix}$$

with entries (in our discrete situation) given by formulas

$$A = \sum_i \sum_j p_x \cdot p_x, B = \sum_i \sum_j p_x \cdot p_y, C = \sum_i \sum_j p_y \cdot p_y$$

we are ready to give explicit formulas for $G(p)$ and $\Theta(p)$, namely,

$$G(p) = (A-C)^2 + 4B^2$$

$$\Theta(p) = \frac{4B^2}{(A-C)^2 + 4B^2}$$

Computing the partial derivates of p_x and p_y using the formulas (1),(2) and (3) above we obtain a Hessian $H_I(p)$. To compute the value of H on p we find the maximum of the absolute values of the eigenvalues of H_I at the central pixel. An explicit formula is given by

$$H(p) = max(|p_{xx} + p_{yy} + \sqrt{(p_{xx} + p_{yy})^2 - 4(p_{xx}p_{yy} - p_{xy})^2}|, \\ |p_{xx} + p_{yy} - \sqrt{(p_{xx} + p_{yy})^2 - 4(p_{xx}p_{yy} - p_{xy})^2}|)$$

The definition of $R(p)$ requires a discrete approximation of continuous basis functions of S. In our representation of patch as a grid Z we achieve this (quite naturally) by evaluating the corresponding basis functions on each of the points of the grid. Once we obtain a discrete model for S we orthonormalize it using the Gram-Schmidt procedure.

Acknowledgments

We gratefully acknowledge the support of DARPA through grant HR 0011-05-1-0007. The work was carried out at the Department of Mathematics at Stanford University.

References

[1] Carlsson G., Ishkhanov T., de Silva V., Zomorodian A. *On the Local Behavior of Spaces of Natural Images.* International journal of Computer Vision (to appear)

[2] Carlsson G., de Silva V. *Topological estimation using witness complexes.* Symposium on Point-Based Graphics (2004)

[3] Singh G., Mémoli F., Ishkhanov T., Sapiro G., Carlsson G., Ringach D. *Topological Analysis of Neuronal Population Activity.* [Submitted]

[4] Edelsbrunner H., Letscher D., Zomorodian A. *Topological persistence and simplification.* IEEE Symposium on Foundations of Computer Science (2000)

[5] Field D.J. *Relations between the statistics of natural images and the response properties of cortical cells.* Journal of the Optical Society of America 4(12) 2379-2394. 1987

[6] Hatcher A. *Algebraic topology.* Cambridge University Press (2001)

[7] van Hateren J.H. *Theoretical predictions of spatiotemporal receptive fields of fly LMCs, and experimental validation.* Journal of Computational Physiology A 171:157-170 (1992)

[8] van Hateren J.H., van der Schaaf A. *Independent component filters of natural images compared with simple cells in primary visual cortex.* Proc.R.Soc.Lond. B 265(1998), 359-366

[9] Knill D.C., Field D.J., Kersten D. *Human Discrimination of Fractal Images.* Journal of the Optical Society of America A, Optics and Image Science, Vol. 7, No. 6. June, 1990

[10] Lee A.B., Pedersen K.S., Mumford D. *The non-linear statistics of high-contrast patches in natural images.* International Journal of Computer Vision 54, 1-3(2003), 83-103

[11] Reinagel P., Zador A.M. *Natural Scene Statistics at the Center of Gaze.* Network: Computation in Neural Systems 10(4) 341-350. November, 1999

[12] de Silva V. *A weak definition of Delaunay triangulation.* (2003)

[13] Silverman B.W. *Density Estimation for statistics and data analysis.* Chapman & Hall/CRC (1986)

[14] Zomorodian A., Carlsson G. *Computing persistent homology.* 20th ACM Symposium on Computational Geometry (2004)